

MICROMECHANICAL SIMULATION OF ASPHALT SAMPLES USING A FINITE ELEMENT NETWORK MODEL

Qingli Dai¹
M. H. Sadd²

ABSTRACT

The micromechanical load transfer and failure of asphalt concrete samples are simulated using a finite element network model. The load carrying behavior of such a material is strongly related to the local load transfer between aggregate particles, and this is taken as the microstructural response. The model incorporates a network of special frame elements with a stiffness matrix developed to predict the load transfer between cemented particle pairs. The stiffness matrix was initially created from an approximate elasticity solution of the stress field in a cementation layer between particles. Continuum damage mechanics was then incorporated within this solution, leading to the construction of a micro-damage model capable of predicting typical global inelastic behavior found in asphalt materials. The finite element micro-model was first used on samples generated from image analysis of actual asphalt material. Using this scheme, simulation models of an indirect tension and a compression sample were generated from surface photographic data of actual laboratory specimens. Simulation results compared favorably with experimental data collected on these samples. An additional series of simulations were also conducted on numerically generated samples with systematic variation of particular microstructure. These results provide comparisons of the effects of microstructure on the overall macro-response on asphalt samples.

Keywords: Asphalt concrete, micromechanical modeling, finite elements.

INTRODUCTION

The micromechanical behavior of asphalt concrete has attracted considerable recent attention. Because of the complex heterogeneous nature of the material (including aggregates, binder and void space), the macro load carrying behavior depends on many micro-phenomena that occur at the aggregate/binder level. Some important micro behaviors are related to binder properties including volume percentage, elastic moduli, inelastic/time-dependent response, aging hardening, microcracking, and debonding from aggregates. Other microstructural features include aggregate size, shape, texture and packing geometry. Because of these issues it appears that a micromechanical model would be best suited to properly simulate such a material. Furthermore, micromechanics offers the possibility to more accurately predict asphalt failure and to relate such

¹ Dept. of Mech. Eng. & Appl. Mech., University of Rhode Island, Kingston, RI 02881, daiq@egr.uri.edu

² Dept. of Mech. Eng. & Appl. Mech., University of Rhode Island, Kingston, RI 02881, sadd@egr.uri.edu

behavior to particular mix parameters such as binder properties, aggregate gradation, and sample compaction.

Recently, many studies have been investigating the micromechanical behavior of particulate, porous and heterogeneous materials. For example, studies on cemented particulate materials by Dvorkin et al. (1994) and Zhu et al. (1996) provided information on the normal and tangential load transfer between cemented particles. Applications of such contact-based micromechanical analysis for asphalt concrete behavior have been reported by Chang and Gao (1997), Cheung, et al. (1999) and Zhu et al. (2000).

Numerical modeling of cemented particulate materials has generally used both finite (FEM) and discrete (DEM) element methods. DEM studies on cemented particulate materials include the work by Rothenburg, et al. (1992), Chang and Meegoda (1993), Trent and Margolin (1994), Buttlar and You (2001), Ullidtz (2001) and Sadd et al. (1998). In regard to finite element modeling, Seppehr et al. (1994) used an idealized finite element microstructural model to analyze the behavior of an asphalt pavement layer. Soares, et al. (2003) used cohesive zone elements to develop micromechanical fracture model of asphalt materials. A particular finite element approach to simulate particulate materials has used an *equivalent lattice network system* to represent the interparticle load transfer behavior. Guddati, et al. (2002) recently presented a random truss lattice model to simulate microdamage in asphalt concrete and demonstrated some interesting failure patterns in an indirect tension test geometry. Bahia et al. (1999) have also used finite elements to model the aggregate-binder response of asphalt materials. Mustoe and Griffiths (1998) developed a finite element model, which was equivalent to a particular discrete element approach.

Damage mechanics provides a viable framework for the description of asphalt stiffness degradation, microcrack initiation, growth and coalescence, and damage-induced anisotropy. Continuum damage mechanics is based on the thermodynamics of irreversible processes to characterize elastic-coupled damage behaviors. Chaboche (1988), Simon and Ju (1987) developed strain- and stress-based anisotropic continuum damage models, and Kachanov (1987) proposed a microcrack-related continuum damage model for brittle materials. These models focus on the relation between damage and effective elastic properties. With respect to asphalt materials, Lee et al. (1998) developed a viscoelastic constitutive model to study the rate-dependent damage growth and damage healing behaviors. Sangpetngam et al. (2003) recently used a displacement discontinuity boundary element approach to simulate the cracking behavior of asphalt mixtures. Papagiannakis (2002) employed imaging techniques to capture the asphalt concrete microstructure and conducted FEM studies for the viscoelastic response.

This paper extends our previous finite element micromechanical modeling of asphalt concrete. Our model incorporates an equivalent lattice network approach whereby the local interaction between neighboring particles is modeled with a special frame-type finite element. The element stiffness matrix is first constructed by using an approximate elasticity solution within the interparticle cementation between particle pairs. Inelastic binder damage behaviors are then simulated by incorporating a continuum damage mechanics theory within the FEM model. This theoretical formulation has then been implemented into the commercial *ABAQUS* FEA code using user-defined elements. Our previous work Sadd, et al. (2001, 2003a,b) applied these modeling procedures on numerically generated asphalt samples with idealized microstructure. The current work explores the use of real asphalt samples to generate the numerical model used in the finite element simulation. To capture the microstructure of real asphalt materials, numerical imaging models were generated from surface scans of actual asphalt specimens. Using image processing, digital photographs of the sample's surface microstructure provided numerical

information for curve fitting algorithms to determine idealized aggregate dimensions and locations. Imaging models of indirect tension and compression specimens were generated for numerical simulation. Comparisons were made of the overall sample behavior and the internal damage pattern between the imaging model and test specimen. Additional FEM simulations were conducted on idealized asphalt samples to investigate particular microstructural influences on the specimen's behavior.

MICROMECHANICAL FINITE ELEMENT MODEL

Asphalt concrete is a heterogeneous cemented particulate material composed of aggregates, binder cement and air voids. The load carrying behavior of such a material is strongly related to the local load transfer between aggregate particles, and this is taken as the microstructural response. Our micromechanical model incorporates an equivalent lattice network approach whereby the local interaction between neighboring particles is modeled with a special frame-type finite element. The element stiffness matrix is constructed by considering the normal, tangential and rotation behaviors between cemented particles, and this is accomplished using an approximate elasticity solution from Dvorkin et al. (1994) for the stress distribution within the cementation interface. Details of the calculation of the various stiffness terms have been reported previously by Sadd and Dai (2001), and the final result is given by

$$[K] = \begin{bmatrix} K_{mn} & 0 & K_{mn}e & -K_{mn} & 0 & -K_{mn}e \\ \cdot & K_u & K_u r_1 & 0 & -K_u & K_u r_2 \\ \cdot & \cdot & K_u r_1^2 + \frac{K_{mn}}{3}(w_2^2 - w_1 w_2 + w_1^2) & -K_{mn}e & -K_u r_1 & K_u r_1 r_2 - \frac{K_{mn}}{3}(w_2^2 - w_1 w_2 + w_1^2) \\ \cdot & \cdot & \cdot & K_{mn} & 0 & K_{mn}e \\ \cdot & \cdot & \cdot & \cdot & K_u & -K_u r_2 \\ \cdot & \cdot & \cdot & \cdot & \cdot & K_u r_2^2 + \frac{K_{mn}}{3}(w_2^2 - w_1 w_2 + w_1^2) \end{bmatrix} \quad (1)$$

where $K_{mn} = (\lambda + 2\mu)w/\bar{h}$, $K_u = \mu w/\bar{h}$, λ and μ are the usual elastic moduli, w and \bar{h} is the average cementation thickness and cementation width, r_1 and r_2 are the radial dimensions from each aggregate center to the cementation boundary, w_1 and w_2 are left and right width of cementation, and $e = (w_2 - w_1)/2$. This procedure establishes the elastic stiffness matrix for each binder element, which is a function of the local material microstructure and binder moduli.

DAMAGE MECHANICS MODEL

To simulate the inelastic damage behaviors observed in asphalt materials, continuum damage mechanics was incorporated within the inter-particle cementation model. The damage stiffness matrix $[D_s]$ can be expressed in terms of the initial elastic stiffness matrix $[D_0]$ using continuum damage principles

$$[D_s] = ([I] - [\Omega])[D_0] \quad (2)$$

and a *damage tensor* $[\Omega]$ is defined by considering the reduction of the effective area of load transfer within the continuum. For the uniaxial inelastic response, the specific constitutive relation is taken as

$$\sigma = \sigma_0(1 - e^{-b(\varepsilon/\varepsilon_0)}) \Rightarrow \frac{\partial \sigma}{\partial \varepsilon} = D_0 e^{-b(\varepsilon/\varepsilon_0)} \quad (3)$$

where the material parameters ε_0 and b are related to the softening strain and damage evolution rate respectively, σ_0 is the material strength, and $D_0 = \sigma_0 b / \varepsilon_0$ is the initial elastic stiffness. Using the damage stiffness definition from relationship (2), the incremental uniaxial damage stiffness D_s and the damage scalar Ω become

$$D_s = (1 - \Omega) D_0 = D_0 e^{-b(\varepsilon/\varepsilon_0)}, \text{ where } \Omega = 1 - e^{-b(\varepsilon/\varepsilon_0)} \quad (4)$$

After critical strength, the softening behavior is taken as

$$\sigma = \sigma_0(1 - e^{-b}) e^{m(1 - \varepsilon/\varepsilon_0)} \Rightarrow \frac{\partial \sigma}{\partial \varepsilon} = -\frac{D_0 m}{b} (1 - e^{-b}) e^{m(1 - \varepsilon/\varepsilon_0)} \quad (5)$$

where m is a material parameter related to the softening rate. The corresponding incremental damage softening stiffness D_s and the damage scalar Ω become

$$D_s = (1 - \Omega) D_0 = -\frac{D_0 m}{b} (1 - e^{-b}) e^{m(1 - \varepsilon/\varepsilon_0)}, \text{ where } \Omega = 1 + \frac{m}{b} (1 - e^{-b}) e^{m(1 - \varepsilon/\varepsilon_0)} \quad (6)$$

The uniaxial stress-strain response corresponding to this particular constitutive model is shown in Fig. 1 for the case of $\varepsilon_0 = 0.2$, $b = 5$ and $m = 1$.

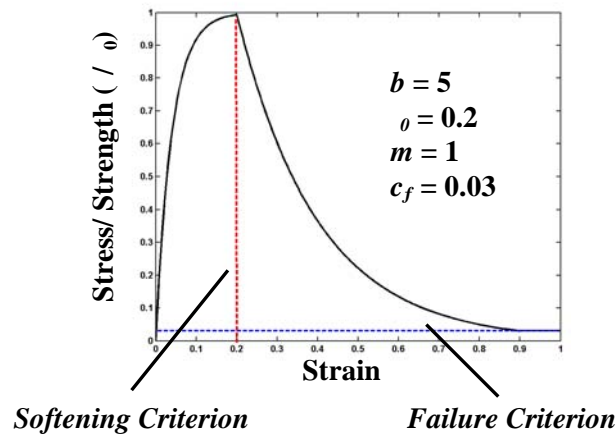


FIG. 1. Uniaxial stress-strain response for damage model

This damage modeling scheme was incorporated into the finite element network model by modifying the micro-frame element stiffness matrix given in Eq. (1). Using the uniaxial relation (4), the incremental normal and tangential damage stiffness terms for the inelastic behavior can be written as

$$(K_{nn})_s = K_{nn} e^{-b(\Delta u_n / \Delta U_n)}, \quad (K_{tt})_s = K_{tt} e^{-b(\Delta u_t / \Delta U_t)} \quad (7)$$

and using Eq. (6) the corresponding incremental normal and tangential damage softening stiffnesses are given by

$$\begin{aligned} (K_{nn})_s &= -(K_{nn} m / b)(1 - e^{-b}) e^{m(1 - \Delta u_n / \Delta U_n)} \\ (K_{tt})_s &= -(K_{tt} m / b)(1 - e^{-b}) e^{m(1 - \Delta u_t / \Delta U_t)} \end{aligned} \quad (8)$$

where Δu_n and Δu_t are the normal and tangential accumulated relative displacements and ΔU_n and ΔU_t are the normal and tangential displacement softening criteria. Thus the micro-frame element incremental damage stiffness matrix $[K_s]$ is constructed from Eq. (1) by replacing K_{nn} and K_{tt} with $(K_{nn})_s$ and $(K_{tt})_s$.

The initiation of binder softening behavior for tension, compression and shear is governed by softening criteria based on accumulated relative displacements between particle pairs

$$\begin{aligned} \Delta U_n^{(t)} &= c_{nt} \bar{h} \\ \Delta U_n^{(c)} &= c_{nc} \bar{h} \\ \Delta U_t &= c_{tt} w \end{aligned} \quad (9)$$

where c_{nt}, c_{nc}, c_{tt} represent tension, compression and shear *softening factors*. These criteria correspond to the average binder critical strength σ_c . Further damage behavior could include evolving microcracking leading to a separation or debonding between aggregate pairs. In order to simulate such total failure, elements were given a binder failure criterion for tension, compression or shear based on the average failure strength σ_f

$$\sigma_f = c_f \sigma_c \quad (10)$$

where c_f is a *failure factor* related to the average failure strength in each behavior, and σ_c indicates the average critical strength in the corresponding behavior. The failure criteria for the uniaxial behavior is also shown in Fig. 1 with the case of $c_f = 0.03$. The failed elements still remain in the computation model, but their stiffnesses are very small and they carry very little load.

IMAGE ANALYSIS OF ASPHALT SAMPLE

In order to capture real asphalt concrete microstructure, simulation material models were generated using imaging analysis procedures from photographic data of actual asphalt samples. The MATLAB Image Toolbox, DIPimage Toolbox and Adobe Photoshop were used for the

image analysis. Surface electronic images were digitally processed and sieved to determine aggregate geometry using a developed image processing code. A least-squares curve-fitting routine was developed within MATLAB and used to numerically fit the best ellipse to each sieved aggregate.

One example image model generation was conducted on a standard 102mm diameter indirect tension sample shown in Fig. 2. A digital camera provided an electronic RGB image of the sectioned specimen, and this was converted to grayscale using Adobe Photoshop as shown in Fig. 2(a). Each grayscale pixel has a brightness value ranging from 0 (black) to 255 (white). A threshold was applied to convert the original images to a binary (black and white), with white signifying the aggregates and black being the combination of binder, air void and aggregate fines that can not be captured by the grid (see Fig. 2(b)). The image size 102×102 mm was digitized to 784×784 pixels, and this results in a 0.13 mm/pixel grid. Next, segmentation techniques were applied to the binary image to ensure that neighboring aggregate pixels did not artificially connect together, see Fig. 2(b). Aggregates were digitally sieved with 50-pixel area size, which lead to a sieving aggregate size less than 1mm. Each sieved aggregate was then labeled and selected as a separate image, and its boundary pixels were extracted and stored in an array for the fitting routine. A least-squares, ellipse-fitting algorithm was then incorporated to determine the “best” ellipse to represent each irregular aggregate geometry. The fitted ellipse was generated for each sieved aggregate as shown in Fig. 2(c), and its geometry (center coordinates, size and orientation) were stored for use in the finite element model generation and simulation.

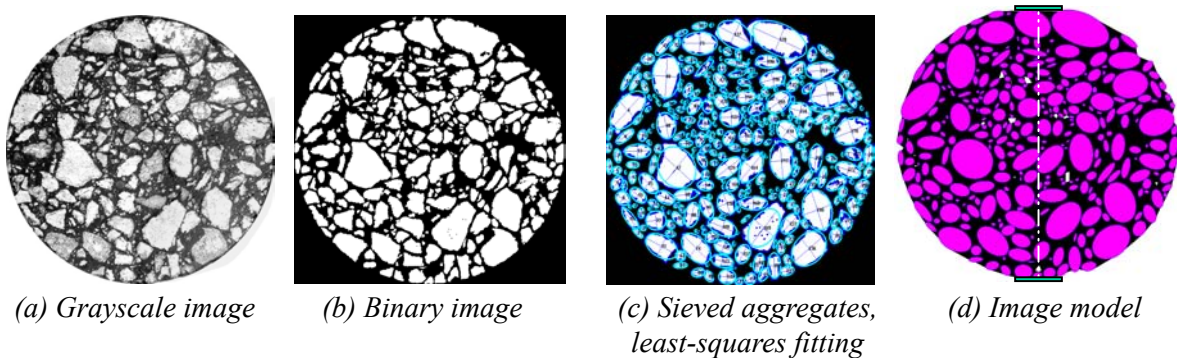


FIG. 2. Image processing and model generation for indirect tension sample

Based on the ellipse parameters obtained from the image analysis, a computation model was generated using MATLAB as shown in Fig. 2(d). Space between neighbor ellipses was maximally filled with cement binder. Once the image asphalt sample was established, the finite element micro-damage model could then be implemented to conduct a loading simulation on the scanned sample. A similar scheme was also used on a rectangular compression sample shown in the next section.

DAMAGE BEHAVIOR SIMULATION ON SCANNED SAMPLES

Simulations of an indirect tension and a compression sample were conducted on the scanned specimens. To model the indirect tension simulation, a special contact boundary condition was imposed on aggregates in contact with the top and bottom loading plates (see Fig.3(a)). The normal contact behavior was simulated by using very stiff elastic finite elements, and a small sliding displacement was allowed between the contact aggregates and the bearing plates to model

frictional behavior. The x - and y -displacements of the bottom plate and x -displacement of top plate were fixed. Sample loading was achieved by incrementing the y -displacement of the top plate. Displacement controlled boundary conditions were also used for the compression simulation (see Fig. 4). For this case the x and y particle displacements of the bottom layer and the x - displacements of particles on the top layer were constrained. The y -displacement loading was incrementally imposed on particles of the top layer.

The model assumes that there exists a continuous distribution of defects in the binder material. This defect field is taken to grow with the material deformation, and this results in a softening response of particular elements in the finite element network. This softening behavior can affect the compression, tension and shear behavior of the element as per Eq. 8, and further softening will lead to binder element failure or fracture. These image models were subjected to incremental loading, and during this process all elements were monitored for softening and failure behavior. Fracture failure patterns and overall load-deformation behavior were compared in the indirect tension test and simulation as shown in Fig. 3. Fig. 3(a) shows the actual damaged specimen from the laboratory test near the end of loading, while Fig. 3(b) illustrates the model fracture pattern in the last loading step by artificially removing the failed elements from the network. There appears to be good agreement between test and simulation results for the fracture patterns in the central portions of the specimen. The model load-deformation behavior also compares favorably with the test data as shown in Fig. 3(c). For the compression test sample, a shear type fracture behavior was observed, see Fig. 4. The experimental result at the end of loading is illustrated in Fig. 4(a) while the model prediction is given in Fig. 4(b). It again appears that the micro-frame damage model has good ability to predict the sample fracture behaviors.

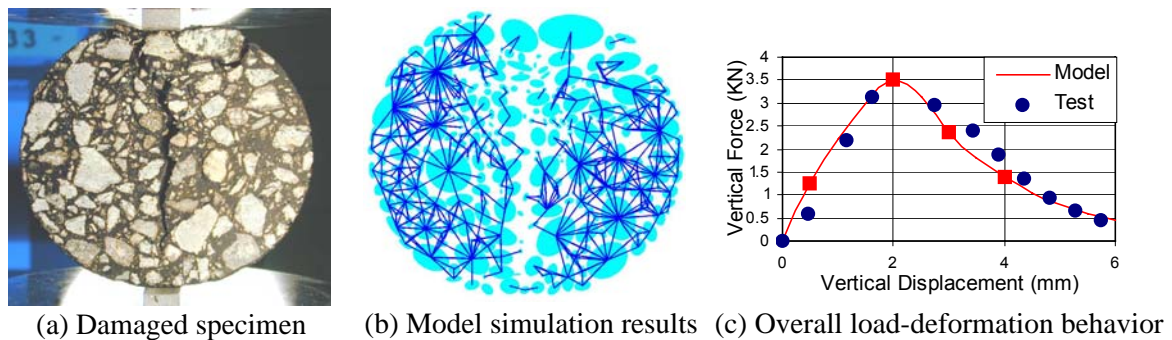


FIG. 3. Fracture patterns and load-deformation behavior comparisons for indirect tension test

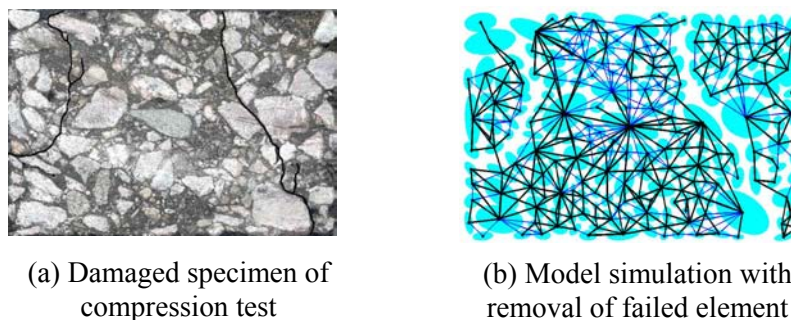


FIG. 4. Fracture patterns in compression test and simulation

MICROSTRUCTURE EFFECTS ON ASPHALT MATERIAL DAMAGE BEHAVIOR

Additional studies included a systematic investigation of the effect of particular microstructural parameters on model simulation results. Typical asphalt microstructural parameters include aggregate gradation, shape, packing fabric, and porosity. A series of model asphalt samples were generated and simulated with controllable microstructure variation in an effort to determine the effect of a particular microstructural variable on the material response. Numerical simulations were conducted on both indirect tension and compression samples, and two examples are shown in Figs. 5 and 6.

Fig. 5 illustrates simulation results for three compression samples with different particle aspect ratios (minor/major axis) of 0.67, 0.8 and 1.0. One actual model is also shown in the figure for the 0.8 aspect ratio case. Model samples for these cases had the same number of particles and elements, identical particle locations and mix percentages, and all samples had zero porosity. The overall simulation response of load vs. sample deformation indicates that samples with smaller aspect ratios generate stiffer global behavior. This appears to happen since the average binder element thickness decreases with decreasing particle aspect ratio, and a lower binder thickness will lead to higher stiffness based on our element equations.

Fig. 6 shows indirect tension simulations on three different models with porosity values (1.1%, 4.6%, 6.7%). The numerical samples were generated using different binder widths and this produces models of variable porosity. The 4.6% porosity model is shown in the figure. As in the previous case, other model micro-parameters such as particle number, size, shape, orientation and percentage were fixed. As the model porosity decreases, the binder element width increases, and this produces a stiffer and stronger finite element model as shown in Fig. 6.

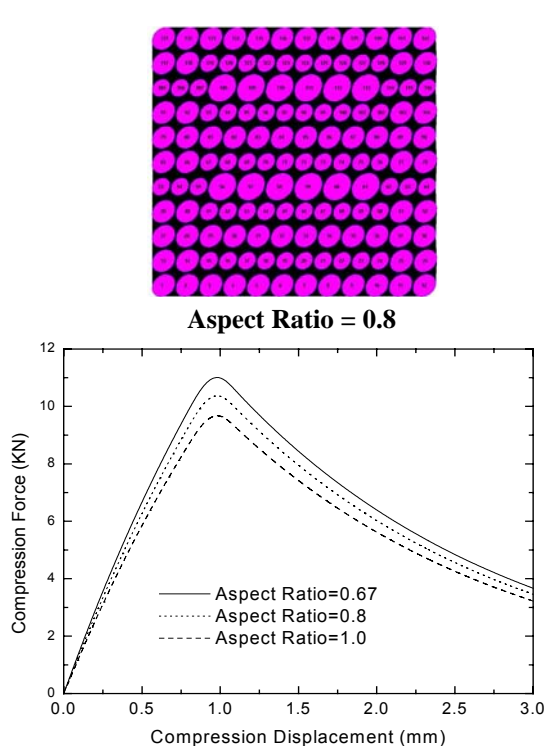


FIG. 5. Compression simulations with different particle aspect ratio

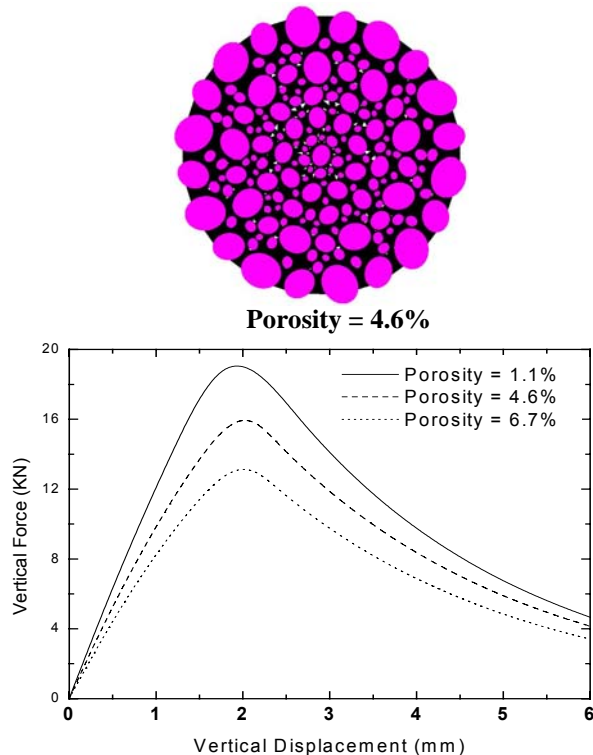


FIG. 6. Indirect tension simulations with different model porosity

CONCLUSIONS

Our previous micromechanical finite element model has been used to simulate the mechanical behavior of asphalt concrete samples. Both indirect tension and compression samples have been investigated under typical laboratory loading conditions. The finite element micro-model was first used on samples generated from image analysis of actual asphalt material. The image analysis scheme allowed a simplified model to be developed from the complex microstructure found in real materials. Using this method, simulation models of an indirect tension and a compression sample were generated from surface photographic data of actual laboratory specimens. Simulation results were then compared with experimental results conducted on the same specimens. Comparisons between model and test data matched reasonably well. Additional simulations were also conducted on numerically generated samples with systematic variation of particular microstructure. These results provided comparisons of the effects of microstructure on the overall macro-response on asphalt samples.

ACKNOWLEDGMENTS

The authors would like to acknowledge support from the Transportation Center at the University of Rhode Island (Grant 03-86). Additional support was also provided from Cardi Construction Corporation.

REFERENCES

- Bahia, H., Zhai, H., Bonnetti, K., and Kose, S. (1999). "Nonlinear Viscoelastic and Fatigue Properties of Asphalt Binders", *J. Assoc. Asphalt Paving Tech.*, 68, 1-34.
- Buttlar, W.G. and You, Z. (2001). "Discrete Element Modeling of Asphalt Concrete: Micro-Fabric Approach", *Transportation Research Record 1757*, TRB, National Research Council, Washington, D.C., 111-118.
- Chaboche, J.L., (1988). "Continuum Damage mechanics, Parts I and II", *International Journal of Applied Mechanics*, 55, 59-72.
- Chang, C.S. and Gao, J. (1997). "Rheological Modeling of Randomly Packed Granules With Viso-Elastic Binders of Maxwell Type", *Comp. and Geotech.*, 21, 41-63.
- Chang, G.K. and Meegoda, N.J. (1993). "Simulation of the Behavior of Asphalt Concrete Using Discrete Element Method", *Proc. 2nd Intl. Conf. On Discrete Element Methods*, M.I.T, 437-448.
- Cheung, C.Y., Cocks, A.C.F., and Cebon, D. (1999). "Isolated Contact Model of an Idealized Asphalt Mix", *Intl. J. Mech. Sci.*, 41, 767-792.
- Dvorkin, J., Nur, A., and Yin, H. (1994). "Effective Properties of Cemented Granular Materials", *Mech.of Materials*, 18, 351-366.
- Guddati, M.N., Feng, Z., and Kim, Y.R. (2002). "Towards a Micromechanics-Based Procedure to Characterize Fatigue Performance of Asphalt Concrete", *Proc. 81st Transportation Research Board Annual Meeting*, Washington, D.C.
- Kachanov, M. (1987). "On Modeling of Anisotropic Damage in Elastic-Brittle Materials-A Brief Review", *Damage Mechanics in Composite*, Ed. Wang, A.S.D., and Haritos, G.K., ASME, 99-105.
- Lee, H.J., and Kim, Y.R. (1998). "Viscoelastic Continuum Damage Model of Asphalt Concrete with Healing", *J. Engng. Mech.*, ASCE, 124(11),1224-1232.
- Mora, P. (1992). "A Lattice Solid Model for Rock Rheology and Tectonics", *The Seismic Simulation Project Tech. Rep.*, 4, 3-28, Institut de Physique du Globe, Paris.

- Mustoe, G.G.W., and Griffiths, D.V. (1998). "An Equivalent Model Using Discrete Element Method (DEM)", *Proc. 12th ASCE Engineering Mechanics Conf.*, La Jolla, CA.
- Papagiannakis, A.T., Abbas, A., and Masad, E. (2002). "Micromechanical Analysis of the Viscoelastic Properties of Asphalt Concretes", *Proc. 81st Transportation Research Board Annual Meeting*, Washington, D.C.
- Rothenburg, L., Bogobowicz, A., and Haas, R. (1992). "Micromechanical Modeling of Asphalt Concrete in Connection with Pavement Rutting Problems", *Proc. 7th Intl. Conf. On Asphalt Pavements*, 1, 230-245.
- Sadd, M.H. and Dai, Q.L. (2001). "Effect of Microstructure on the Static and Dynamic Behavior of Recycled Asphalt Material", *Year 1 Final Report #536108*, University of Rhode Island Transportation Center.
- Sadd, M.H., Dai, Q.L., Parameswaran, V., and Shukla, A. (2003a). "Microstructural Simulation of Asphalt Materials: Modeling and Experimental Studies", to appear in *ASCE Jour. of Materials in Civil Eng.*
- Sadd, M.H., Dai, Q.L., Parameswaran, V., and Shukla, A. (2003b). "Simulation of Asphalt Materials Using a Finite Element Micromechanical Model and Damage Mechanics", *Proc. 82nd Transportation Research Board Annual Meeting*, Washington, D.C.
- Sadd, M.H., and Gao, J.Y. (1998). "Contact Micromechanics Modeling of the Acoustic Behavior of Cemented Particulate Marine Sediments", *Proc. 12th ASCE Engineering Mechanics Conf.*, La Jolla, CA.
- Sangpetngam, B., Birgisson, B., and Roque, R. (2003). "Development of an Efficient Hot Mix Asphalt fracture Mechanics-Based Crack Growth Simulator", *Proc. 82nd Transportation Research Board Annual Meeting*, Washington, D.C.
- Sepehr, K., Harvey, O.J., Yue, Z.Q., and El Husswin, H.M. (1994). "Finite Element Modeling of Asphalt Concrete Microstructure", *Proc. 3rd Intl. Conf. Computer-Aided Assessment and Control Localized Damage*, Udine, Italy.
- Simon, J. C., and Ju, J. M. (1987). "Strain- and Stress-Based Continuum Damage Models I. Formulation", *Intl. J. Solids Structures*, 23(7), 821-840.
- Soares, J.B., Colares de Freitas, F.A. and Allen, D.H. (2003) "Crack Modeling of Asphaltic Mixtures Considering Heterogeneity of the Material", *Proc. 82th Transportation Research Board Meeting*, Washington, D.C.
- Trent, B.C., and Margolin, L.G. (1994). "Modeling Fracture in Cemented Granular Materials", *Fracture Mechanics Applied to Geotechnical Engineering*, ASCE Pub., *Proc. ASCE National Convention*, Atlanta.
- Ullidtz, P. (2001). "A Study of Failure in Cohesive Particulate Media Using the Discrete Element Method", *Proc. 80th Transportation Research Board Meeting*, Washington, D.C.
- Zhu, H., Chang, C.S., and Rish, J.W. (1996). "Normal and Tangential Compliance for Conforming Binder Contact I: Elastic Binder", *Intl. J. Solids Structures*, 33, 4337-4349.
- Zhu, H., and Nodes, J.E. (2000). "Contact Based Analysis of Asphalt Pavement with the Effect of Aggregate Angularity", *Mech. of Materials*, 32, 193-202.